Machine Learning in Prediction of Prostate Brachytherapy Rectal Dose Classes at Day 30

P. Leydon[1,2], F. Sullivan[2], F. Jamaluddin[2], P. Woulfe[2], D. Greene[3], K. Curran[1].

[1]*School of Medicine & Medical Science, University College Dublin, Ireland*

[2]*The Galway Clinic Ireland*

[3]*School of Computer Science & Informatics, University College Dublin, Ireland*

Abstract

A retrospective analysis of brachytherapy implant data was carried out on 351 patients that underwent permanent I^{125} brachytherapy for treatment of low-risk prostate cancer. For each patient, the dose received by $2cm^3$ of the rectum (D2cc) 30 days post implant was defined as belonging one of two classes, "Low" and "High" depending on whether or not it was above or below a particular dose threshold. The aim of the study was to investigate the application of a number of machine learning classification techniques to intra-operative implant dosimetry data for prediction of rectal dose classes determined 30 days post implant. Algorithm performance was assessed in terms of its true and false positive rates and Receiver Operator Curve area based on a 10-fold cross validation procedure using Weka software. This was repeated for a variety of dose class thresholds to determine the point at which the highest accuracy was achieved. The highest ROC areas were observed at a threshold of D2cc = 90 Gy, with the highest area achieved by Bayes Net (0.943). At more clinically useful thresholds of D2cc = 145 Gy, classification was less reliable, with the highest ROC area achieved by Bayes Net (0.613).

Keywords: Brachytherapy, Prostate Cancer, Machine Learning, Classification, Weka.

1 Introduction

Prostate cancer is the second most frequently diagnosed cancer and the sixth leading cause of cancer death in males, accounting for 14% (903,500) of the total new cancer cases and 6% (258,400) of the total cancer deaths in males in 2008 [Jemal et al., 2011].

The permanent transperineal interstitial placement of I^{125} seeds is a popular choice for Low Dose Rate Brachytherapy of Prostate Cancer. The deposited-seed positions are imaged and the plan optimized in real-time throughout the procedure. The dose distribution is updated dynamically based on the actual positions as the seeds are deposited. The clinical and technological improvements that have emerged over the last decade in low dose rate prostate brachytherapy such as the use of ultrasound and computed tomography-based treatment planning systems has led to a resurgence in the use of the technique for localized prostate cancer [Jemal et al., 2011].

As prostate cancer is being diagnosed at increasingly early stages, quality-of-life issues when choosing the primary treatment modality are becoming of greater concern. Prostate brachytherapy has many advantages over both external-beam radiation therapy and radical prostatectomy, however it has been shown that because the rectum often receives a large radiation dose this may lead to radiation-induced rectal injury such as rectal

 ISBN 978-0-9934207-0-2

bleeding, chronic radiation proctitis which if not managed correctly can result in fistula development and the eventual need for a colostomy.

With regards to rectal dosimetry, the guidelines given by Snyder et al based rectal dose constraints on an annular dose-volume histogram of the rectum, aiming to achieve less than 160 Gy to 1.3 cm^3 for I^{125} monotherapy. This rule is often modified by practitioners who prescribe 145 Gy minimum peripheral dose (mPD), and for doses to 2.0 cm^3 of the rectum to be less than 145 Gy [Nath et al., 2009].

Due to the permanent nature of the implant the dose is determined by integrating the dose rate from the time of implantation until the isotope has decayed to background levels, taking into account the physical decay of the sources only and assuming that the geometry of implant and anatomy established at the date of scan does not change over time.

To account for this time variance in prostate volume, seed position and the subsequent dosimetry calculations, the post-implant CT scan is often postponed for approximately 1 month after the procedure assuming that the prostate volume, seed positions etc will change very little afterwards [Steggerda et al., 2007]. Changes in rectal doses have been observed between measurements made intraoperatively and from a patient's post-implant CT. The differences have been largely attributed to changes in rectal proximity to the implanted seeds as periprostatic edema resolves [Nag et al., 1999]. Discrepancies in rectal doses may also be as a consequence of the different patient set-ups and the resulting variation in prostate positions during intra-operative transrectal ultrasound (dorsal lithotomy position) and postplanning CT (supine position) [Pinkawa et al., 2009].

The aim of the study was to investigate the application of machine learning techniques to intra-operative implant dosimetry data for prediction of rectal dose classes determined 30 days post-implant.

2 Methods

A retrospective analysis of brachytherapy implant data was carried out on 351 patients that underwent permanent I^{125} brachytherapy for low-risk prostate cancer. For each patient, the dose received by 2 cm^3 of the rectum (D2cc) at day 30 was defined as belonging to one of two classes, Low <(Dose Threshold), and High >(Dose Threshold). The original dataset, n = 351, contained approximately 40 intra-operative measurements which was then reduced to a selection of 10 predictors, using the "Best First" method in Weka [Hall et al., 2009]. Any data with missing values were excluded, leaving the final refined set of n = 347. The day 0 predictors used in this study were, (i) Treatment Type, (ii) Pre-Needle Prostate Volume, (iii) Post-Needle Prostate Volume, (iv) Dose to 90% of the Prostate (D90), (v) Minimum Dose to Prostate, (vi) Mean Dose to Prostate, (vii) Dose to 30% of the urethra (U30), (viii) Dose to 10% of the urethra (U10), (ix) Dose to 5% of the urethra (U5), and (x) the dose to 2 cm^3 of the rectum (D2cc).

Variable	Value ± SD	Range
Age	63.41 ± 6.99	42.07 - 83.27
Prostate Volume cc	33.47 ± 10.96	11.5 - 62
Treatment Type	Mono(258), Boost(83),	Salvage(10)
Activity per seed	0.51 ± 0.04	0.35 - 0.58
Total Activity mCi	27.37 ± 8.68	9.26 - 84
Number of Seeds	66.83 ± 16.23	26 - 105
Number of Needles	17.95 ± 2.84	10 - 25
Initial PSA ng/ml	7.61 ± 3.70	1.5 - 29
Gleason		(3+1) - (5+5)
ADT	~28%	
Pre Needle Volume cc	31.06 ± 10.62	10.23 - 62.3
Post Needle Volume cc	32.91 ± 11.91	11.4 - 64.7
D90 Day 0	155.30 ± 24.89	85.96 - 192.34
Minimum Dose Day 0	97.72 ± 22.08	11.62 - 179.18
Mean Dose Day 0	230.64 ± 32.89	155.49 - 284.53
U30 Day 0	163.48 ± 26.73	12.06 - 220.69
U10 Day 0	172.128 ± 27.48	110.44 - 248.24
U5 Day 0	175.92 ± 28.78	112.53 - 267.4
D2cc Day 0	82.41 ± 25.37	23.36 - 160.47
D2cc Day 30	111.29 ± 28.28	22.46 - 190.95

Figure 1: Patient dataset summary statistics.

Changes of dose distribution for both the prostate and the surrounding tissues after brachytherapy have been reported in literature, and have been largely attributed to factors such as edema, intra-observer variability, and the use of different imaging modalities with different patient set-up between day 0 and day 30 [Moorrees et al., 2012]. In Figure 2. these changes in rectal doses between day 0 and day 30 are evident, with an obvious overall shift towards higher rectal doses at day

 ISBN 978-0-9934207-0-2

30.

Machine learning techniques, developed using Weka software, were trained on the refined dataset to make predictions of rectal dose classification at day 30. Four algorithms were used;
(i) **Radial Basis Function network (RBF)** - Implements a normalized Gaussian radial basis function network, with k-means clustering algorithm providing the basis functions for logistic regression. Symmetric multivariate Gaussians are fit to the data from each cluster. All numeric attributes are standardized to zero mean and unit variance.
(ii) **J48** - A pruned decision tree based on the C4.8 algorithm [Quinlan, 1993]. The number of folds used was 3, with subtree raising when pruning, and without binary splits on numeric data or Laplace smoothing.
(iii) **Random Tree** - Constructs a desecion tree that considers a number of randomly chosen attributes at each node. No pruning, and no backfitting was performed.
(iv) **BayesNet** - Uses the K2 hill climbing algorithm restricted by the Weka default variables. The maximum number of parents in the Bayes Net was set to 1, resulting in a Naive Bayes classifier. Conditional probabilites were determined by selecting the Simple Estimator option with alpha = 0.5.

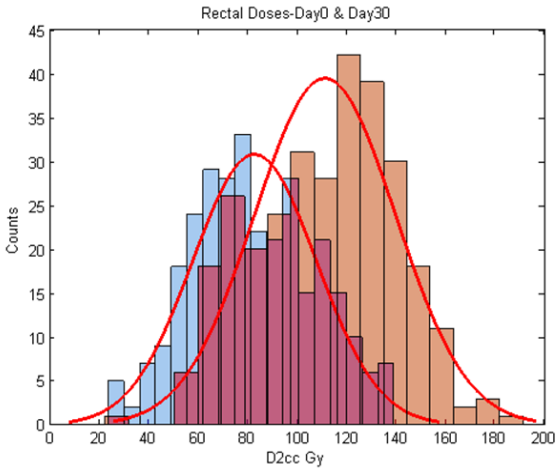

Figure 2: Patient dataset summary statistics.

The performance of a technique was assessed in terms of true and false positive rates, and area under Receiver Operator Curves based on a 10-fold cross validation procedure. This process was repeated for a number of different thresholds ranging from D2cc of 50 Gy to 180 Gy in order to determine the point at which an algorithm demonstrated the highest accuracy.

3 Results

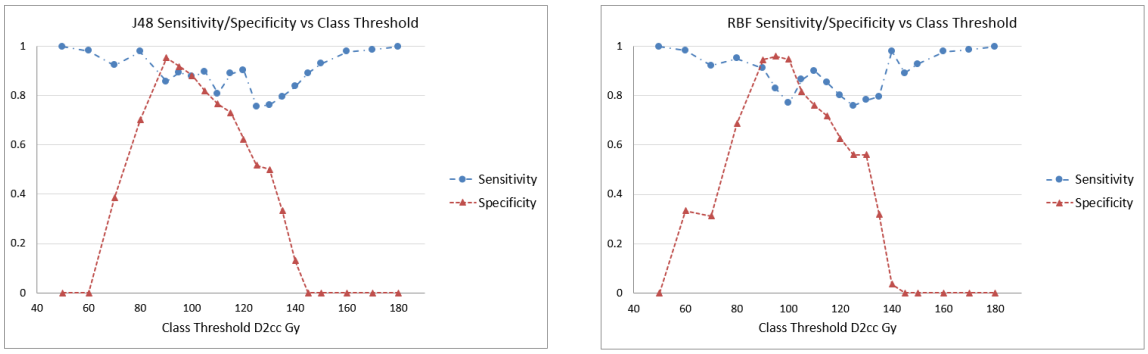

Figure 3: Shows both sensitivity and specificity results for J48 and Radial Basis Function algorithms at various dose thresholds.

The four algorithms displayed a similar performance overall in the threshold ranges tested, with similar changes in sensitivity and specificity clearly visible in Figures 3 & 4. The ROC areas in Figure 5 demonstrate the variation across the threshold range depending on the choice of algorithm; however all appear to give the

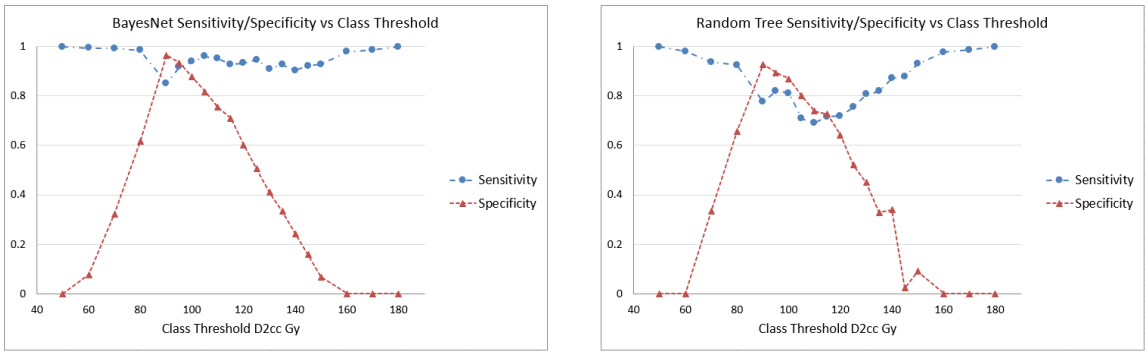

Figure 4: Shows both sensitivity and specificity results for BayesNet and Random Tree algorithms at various dose thresholds.

best result close to a threshold of 90 Gy, with ROC areas of 0.928 (J48), 0.927 (Radial Basis Function), 0.943 (BayesNet), and 0.851 (Random Tree). At the more clinically important threshold of 145 Gy algorithms display considerably less accuracy with ROC areas of 0.477 (J48), 0.660 (BayesNet), 0.613 (Radial Basis Function), and 0.444 (Random Tree).

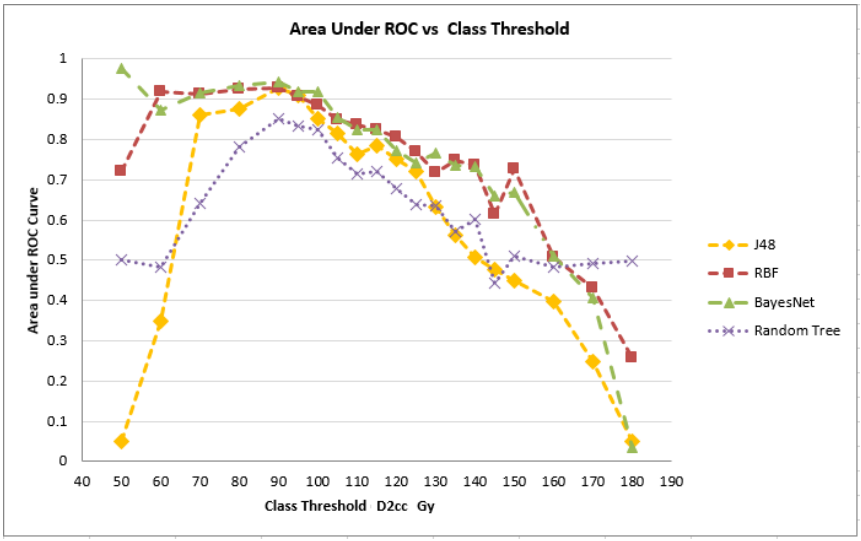

Figure 5: Reciever Operator Curves for all four algorithms.

4 Conclusion

All four of the algorithms appear to predict reliably at a rectal dose threshold of approximately 90 Gy. However, it is prediction at the higher dose thresholds that would be of most use in a clinical setting but as the rectal dose class threshold passes the 90 Gy mark predictions become steadily less reliable.

It may be worth exploring the effect that inclusion, or exclusion of combinations of the 10 predictor variables used in this study has on the accuracy of the algorithms. Some predictors may not be necessary for optimum training of algorithms and may be impeding reliable classification. The possible inclusion of any outliers in training data may also be reducing performance.

It has been by shown that implant variables, such as D90, do not depend on the post-implantation date of the scan supplying the images for dosimetry however some parameters associated with morbidities strongly changed within the first month after implantation, meaning that the time at which a scan is carried out may be an important variable to consider and one which was not included as part of this study [Steggerda et al., 2007].

Weka provides a much larger selection of classification algorithms than the four used in this study, such as Mutli Layer Perceptrons and Support Vector Machines. It may be that one of these other algorithms is more suited to this particular classification task, than those that were used. The inclusion of uncertainties associated with classification predictions would also be of use clinically.

References

[Hall et al., 2009] Hall, M., Frank, E., Holmes, G., Pfahringer, B., Reutemann, P., and Witten, I. H. (2009). The weka data mining software: An update. *SIGKDD Explor. Newsl.*, 11(1):10–18.

[Jemal et al., 2011] Jemal, A., Bray, F., Center, M. M., Ferlay, J., Ward, E., and Forman, D. (2011). Global cancer statistics. *CA: a cancer journal for clinicians*, 61(2):69–90.

[Moorrees et al., 2012] Moorrees, J., Lawson, J. M., and Marcu, L. G. (2012). Assessment of i-125 seed implant accuracy when using the live-planning technique for low dose rate prostate brachytherapy. *Radiation Oncology*, 7(1):196.

[Nag et al., 1999] Nag, S., Beyer, D., Friedland, J., Grimm, P., and Nath, R. (1999). American brachytherapy society (abs) recommendations for transperineal permanent brachytherapy of prostate cancer. *International Journal of Radiation Oncology* Biology* Physics*, 44(4):789–799.

[Nath et al., 2009] Nath, R., Bice, W. S., Butler, W. M., Chen, Z., Meigooni, A. S., Narayana, V., Rivard, M. J., and Yu, Y. (2009). Aapm recommendations on dose prescription and reporting methods for permanent interstitial brachytherapy for prostate cancer: Report of task group 137. *Medical physics*, 36(11):5310–5322.

[Pinkawa et al., 2009] Pinkawa, M., Asadpour, B., Piroth, M. D., Gagel, B., Klotz, J., Fischedick, K., Borchers, H., Jakse, G., and Eble, M. J. (2009). Rectal dosimetry following prostate brachytherapy with stranded seeds–comparison of transrectal ultrasound intra-operative planning (day 0) and computed tomography-postplanning (day 1 vs. day 30) with special focus on sources placed close to the rectal wall. *Radiotherapy and Oncology*, 91(2):207–212.

[Quinlan, 1993] Quinlan, J. R. (1993). *C4.5: Programs for Machine Learning*. Morgan Kaufmann Publishers Inc., San Francisco, CA, USA.

[Steggerda et al., 2007] Steggerda, M. J., Moonen, L. M., van der Poel, H. G., and Schneider, C. J. (2007). The influence of geometrical changes on the dose distribution after i-125 seed implantation of the prostate. *Radiotherapy and oncology*, 83(1):11–17.